Eyelid Measurements Using Digital Video Processing

Carlos Hitoshi Morimoto
Department of Computer Science
University of São Paulo
Rua do Matão, 1010 - SP - Brazil
hitoshi@ime.usp.br

Thomaz Fracon de Oliveira
Department of Ophthalmology
University of São Paulo
Av. Dr. Enéas de C. Aguiar, 255 - SP - Brazil
fracon@bhoftalmo.com.br

ABSTRACT

The aim of this paper is to present an automatic eyelid measurement system based on digital video processing techniques. Currently, the protocol to measure the palpebral fissure (PF) and the marginal reflex distance (MRD) requires the use of a millimetric ruler. This procedure is subject to error and the accuracy and reproducibility of the results depend on the experience of the examiner. The computer vision system introduced in this paper uses two near infrared light sources synchronized with the camera to robustly detect and track the pupil, and then segment the limbus and the eyelids. The corneal reflection generated by the light sources are used to create a reference point that is used to define the vertical line along which the measurements are taken, and to determine when the patient is actually looking at the camera. Our experimental results show that the system is robust to the presence of eyelashes, glasses, and contact lenses, and the measurements can be accurate to tenths of millimeters.

Categories and Subject Descriptors

J.3 [**Computer Applications**]: Life and Medical Sciences; I.4 [**Computing Methodologies**]: Image Processing and Computer Vision—*eye tracking, eyelid measurements*

Keywords

Eye detection, eye tracking, eyelid measurements.

1. INTRODUCTION

A thorough palpebral (eyelid) exam can reveal several pathological conditions caused by congenital, myocongenic, neurological, neoplastic and/or traumatic processes. The eyelid exam starts with the collection of the patient history of present illness to acquire data such as the duration of the condition, evolution, associated signs and symptoms, predisposition factors, preceding treatments and the patient's family history [14, 6]. A complete ophthalmological exam follows. It consists of measuring visual acuity, refraction, papillary responses, neurosensory exam, evaluation of eyebrows, upper and lower eyelid, ocular motility, biomicroscopy, ophthalmoscopy and tonometry [13]. At the end, the case is documented using photographs that can be used for pos-surgery comparison, legal purposes, and as scientific evidence [5].

The common protocol to obtain eyelid measurements is to measure distances against a ruler. Figures 2 and 3 show pictures of eyes during the examination. Sometimes, pictures of the eyes are taken so that the measurements can be computed from the images later. These measurements are used to characterize the severity of the pathology and guide the ophthalmologist to choose the appropriate surgical procedure [14].

As reported in [2], although the repeatability and reproducibility of the measurements are clinically acceptable when the technique of assessment is standardized, there is a learning curve associated with the experience of the examiner.

In this paper we introduce a computer vision technique to automate this process. We have developed a device to detect and track the pupil and corneal reflections robustly, measure their image position and sizes using automatic image processing techniques, and show how to compute the eye measurements after a calibration procedure. The next section describe the eye structure and the simplified model that is used to compute the measurements. Section 3 describes the procedure to obtain some common palpebral metrics, and Section 4 introduces our computer vision system that automatically measures the Palpebral Fissure and the Marginal Reflex Distance from the video camera. Experimental results are presented in Section 5 and Section 6 concludes the paper.

2. EYE STRUCTURE

The eye has an approximately spherical shape with a radius of about 12 mm [15]. The external parts of the eye that are visible in the eye socket are the sclera (the white part of the eye), the iris (the color part of the eye), and the pupil located in the center of the iris. The cornea is a transparent tissue, with a highly organized group of cells and proteins, with no blood vessels, that protrudes toward the front of the eye, covering the iris. It is constantly lubricated by tears during blinking. The limbus is the transition between the sclera and the cornea. In a healthy person, the upper eyelid covers the cornea about 2 mm below the upper limbus and the lower eyelid passes tangently the inferior limbus.

The eyelid is composed of protractor and retractor mus-

SAC'08 March 16-20, 2008, Fortaleza, Ceará, Brazil

cles. Protractor muscles are activated to close the eyelid, and retractor muscles to open. The protractor muscles are represented by the orbicularis oculi muscles. The upper eyelid retractor are the muscle of Mller and the levator palpebrae superioris muscle. The lower eyelid retractors are the capsulopalpebral fascia and the inferior tarsal muscles [7, 9].

The iris controls the pupil size by the action of its dilator and sphincter muscles. Its complex fibrillous pattern is due to the elastic connective tissue that constitute these muscles.

Figure 1 shows our simplified 2D model of the eye, roughly defining the surfaces that are segmented in this study. The iris region is defined by two boundary circles, the inner circle that corresponds to the boundary of the pupil and iris, and an outer circle on the boundary of the iris and the sclera, called limbus. Observe that the position of the upper and lower eyelids are arbitrary in this model, they may or may not occlude the iris, and, although the inner and outer circles of the iris are not concentric, the distance between their centers is not significant in this model.

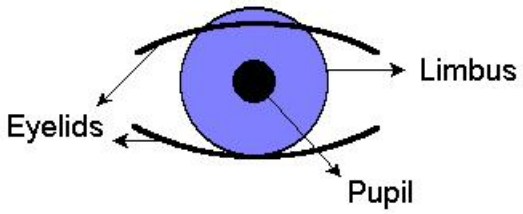

Figure 1: Simplified 2D eye model. It contains the iris region, defined by the inner (pupil) and outer (limbus) circles of the iris, and the upper and lower eyelids.

3. EYE MEASUREMENTS

As described earlier, the palpebral evaluation consists of a thorough examination to collect data and measurements using a ruler. Boboridis *et al.* [2] studied the repeatability and reproducibility of upper eyelid measurements when following a standard protocol to measure three basic measurements: marginal reflex distance (MRD) for upper and lower lids, upper slid skin crease (SC), and levator function (LF). The procedures are as follows:

- MRD measurement: the patient is requested to look at a light source and distances from the corneal reflection to the upper and lower eyelids are recorded.
- SC measurement: the patient is asked to look down, the upper lid skin fold is gently raised if necessary, and the distance of the skin crease from the eyelid margin is recorded.
- LF measurement: the patient's eyebrow is first stabilized by pressure exerted with the examiner's thumb and then asked to look fully up, then fully down, while the excursion of the eyelid is measured against a ruler. This procedure is repeated three times and the average measurement is recorded.

For each measurement, the examiner must sit in front of the patient at the same level and both look in the primary position. Their results suggest that interobserver and intraobserver variability in assessment of upper lid ptosis using this protocol was low and clinically acceptable. Figure 2 shows how the upper MRD is measured.

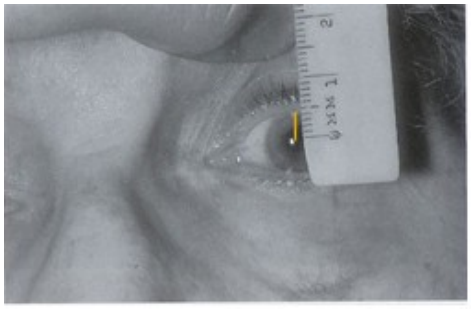

Figure 2: Upper marginal reflex distance (MRD) measurement.

Another commonly used measurement is the palpebral fissure (PF), defined as the region delimited by the upper and lower eyelids. The procedure measures the distance between eyelids, when patient and examiner are looking in the primary position, along an imaginary vertical line crossing the pupil center. Figure 3 illustrates how the PF is measured.

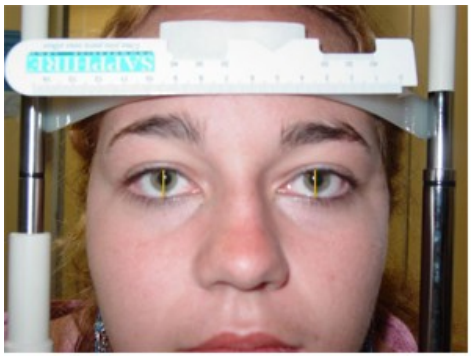

Figure 3: Palpebral fissure (PF) measurement.

4. DIGITAL VIDEO PROCESSING

There is a vast literature about eye detection and tracking. A recent surveys about eye tracking is given by Duchowski [4]. Applications range from eye as an input mode in computer interfaces, iris identification, to neuroscience experiments to investigate eye behavior. Image processing has been demonstrated to be a reliable tool to compute palpebral measurements [3]. The method was not fully automated though, and because the results are computed from static pictures (not a video) taken from a high resolution camera, the picture must be carefully taken to avoid blinks, gaze direction, interference from eyelashes, etc. Our technique is able to detect when the patient is looking at the camera, so the correct measurement can be taken.

The first step to capture a good image of the eye is to control the illumination conditions. We use two near infrared (NIR) light sources to facilitate pupil detection and eye feature segmentation. Once the position and size of the

pupil is computed, the iris and eyelids are segmented using a coarse-to-fine multiresolution strategy. Figure 4 shows the block diagram of our eye feature segmentation technique.

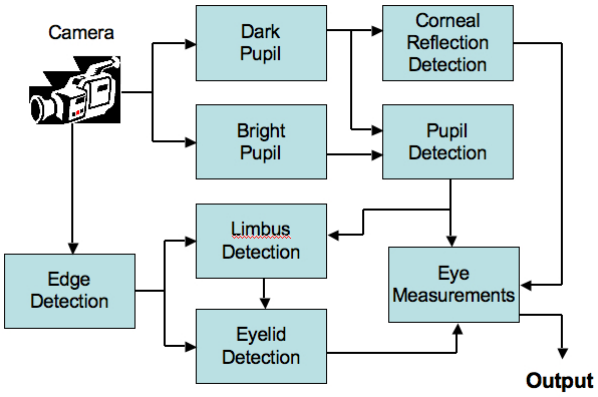

Figure 4: Block diagram of the eye feature measurement system.

The two NIR light sources are combined similarly to the eye tracking systems described by Morimoto *et al.* [10]. An NIR light source placed near the optical axis of a black and white NTSC camera generates a bright pupil image, as seen in Figure 5a. The bright pupil effect is a well known phenomenon from night flash photography, and many cameras today have settings to reduce the "red" pupil effect. The second light source placed far from the optical axis of the camera generates a dark pupil image, as seen in Figure 5b. These two light sources can be synchronized with the even and odd frames of the B&W NTSC video camera that captures the eye image. From the subtraction of these two frames, the pupil, as the larger connected region of high contrast, can be easily segmented.

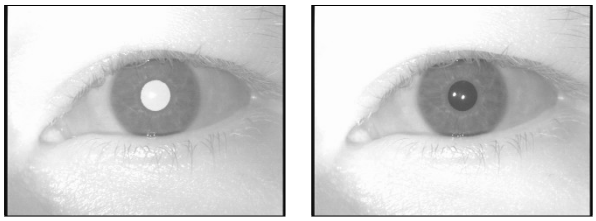

(a) (b)

Figure 5: (a) bright; (b) dark pupil images. Observe that the pupil can be easily segmented using the high contrast regions.

The corneal reflections correspond to bright spots, that can be seen at the center of the pupils in Figure 5. Bright spots may appear on the corners of the eye, particularly when the eye is well lubricated with tears. Because we use the corneal reflections to determine when good quality images can be used for measurements, the algorithm searches for bright pixels near the center of the pupil region. When bright pixels are detected near the pupil center, the images are further processed to segment the limbus and eyelids. The dark pupil image is used to detect the corneal reflection due to the better contrast.

4.1 Segmentation of the limbus and eyelids

Once the size and position of the pupil is computed from two consecutive frames of the video signal, the limbus and eyelids are segmented using a coarse-to-fine multi-resolution strategy. Since the sclera is predominantly white, the gradient around the iris-sclera boundary points towards the sclera [8]. The knowledge of the expected direction of the gradient is used to fit the external circle around the iris.

Horizontal and vertical image gradients can be computed using the Sobel operator. Since the iris can be occluded by the eyelids, the best edge points to fit the limbus circle are the vertical edges. Therefore, only the strong gradients in the horizontal direction are used to fit the limbus. We also know that the filter returns strong negative values on the left boundary region of the limbus, and strong positive values on the right boundary. Figure 6 show the result of multi-resolution algorithm to segment the iris and the eyelids.

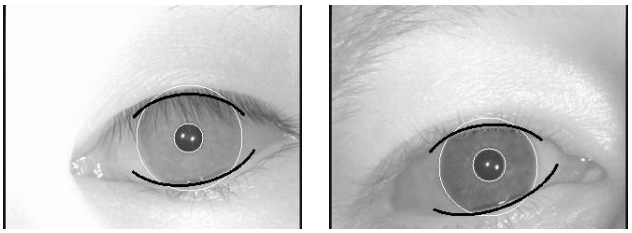

Figure 6: Results of the multi-resolution algorithm that segments the iris and the eyelids.

We assume a similar hypothesis to fit ellipses for the eyelids, i.e., the best edge points for the eyelids are mostly horizontal, and therefore, only the strong gradients along the vertical direction are used to fit the eyelids. We also know that the filter returns strong positive values for the upper eyelid, and strong negative values for the lower eyelid.

The iris segmentation starts by building a Gaussian pyramid of the input image. Edge detection using Canny's algorithm, that returns thin edges, is applied to all pyramid levels to create an edge pyramid. Examples of an image pyramid and an edge pyramid are shown in Figure 7. Observe that at the coarsest levels of the pyramid, the high frequency components that correspond to small details of the image such as noise and eyelashes are filtered out.

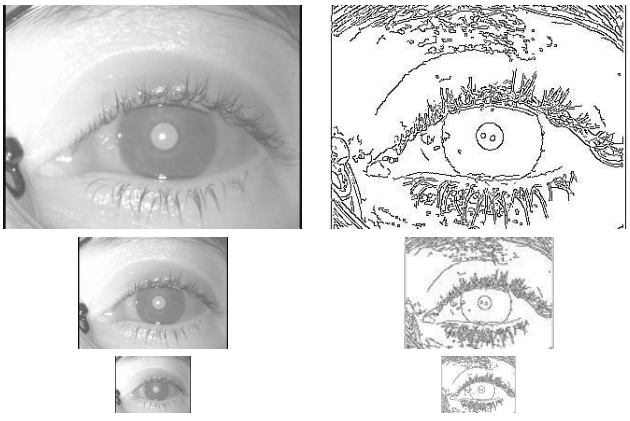

Figure 7: Image and edge pyramids.

The search for the outer circle starts at the coarsest level of the edge pyramid, around a search box centered at the pupil. Edge points to the left with strong negative responses of the horizontal Sobel mask, and edge points to the right of the search box with strong positive responses are used to fit a circle. Once the circle is estimated for the lowest pyramid resolution, it is refined using the next finer resolution pyramid level.

The eyelids are segmented in a similar coarse-to-fine strategy, after the segmentation of the iris. The position and size of the iris defines a search box for the upper and lower eyelids at the lowest resolution of the edge pyramid. All pixels inside the iris are automatically discarded, and only the edge points with strong negative or positive responses from the vertical Sobel mask are used to fit the ellipses for the eyelids.

4.2 PF and MRD estimation

The corneal reflection as seen in Figures 2 and 3 provides the examiner a reference point to measure the MRD and PF. The use of near infrared light makes the examination more comfortable to the patient since it is practically invisible to the human eye.

For our system, the corneal reflection is also used to indicate when the patient is looking in the primary position. Figure 8 shows the geometry of the image acquisition using the NIR light sources. The center of the camera, eye and light source define a plane. The acquisition camera and light sources can be placed at the patient's eye level with the help of a chin or head rest as seen in Figure 3. When looking in the primary position the patient looks straight at the camera. This situation can be automatically detected by the system since the corneal reflection, as shown in Figure 8 appears in the center of the pupil. If the patient is not looking in the primary position, his/her pupil will move and the measurements will not be computed. This idea was also explored in [1] to detect eye contact of the user with the pupil detector, and in [11] for iris segmentation.

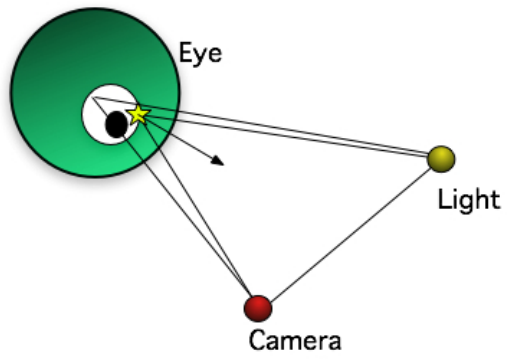

Figure 8: Geometry of the camera, eye and light sources. The center of the camera, light and eye define a plane. Observe that, when the eye looks at the light source placed near the camera, the corneal reflection (represented by a little start on the surface of the cornea), the reflection lies in the center of the pupil.

5. EXPERIMENTAL RESULTS

Figure 9 shows some results from the segmentation of the pupil, iris, and corneal reflection (represented by the crosshair), using the hierarchical technique presented earlier. The camera and NIR light sources were placed about 50cm from the patient's face. Note that the top left image in Figure 9 shows that the detection technique works also when the patient is wearing glasses, and the top right image shows a particular case of an eye with long eyelashes that covers a significant part of the iris and sclera. The contrast around the iris were digitally enhanced to facilitate the visualization of the results.

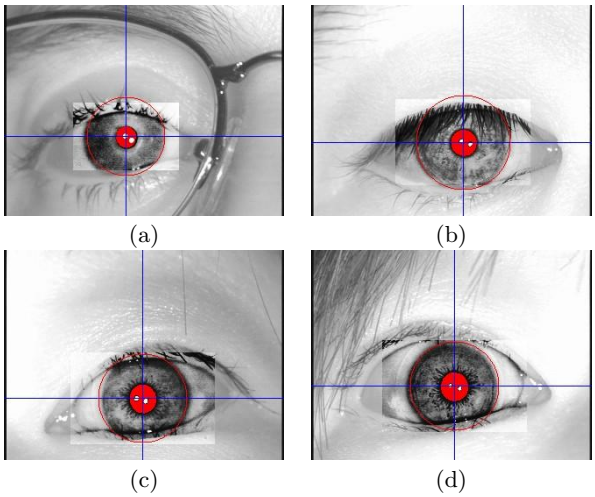

Figure 9: Results from the pupil, iris, and corneal reflection segmentation. (a) person with glasses; (b) eyelashes are covering large part of the iris and sclera, (c) normal eye; and (d) eye with contact lenses.

Figure 10 shows some results for the segmentation of the eyelids for the PF and MRD measurements. The extension in pixels of the vertical line that contains the corneal reflection in the center of the pupil, from the lower to the upper lid, corresponds to the PF. The distance from the corneal reflection to the upper and lower lids define the uMRD and lMRD respectively, in image pixels. To convert the measurements from pixels to millimeters, a picture of a ruler was taken and used as reference (200 pixels in the vertical direction correspond to 10mm). Table 1 shows the actual measurements in pixels and in millimeters (the first number is the measurement in pixels, and the second is converted to millimeters).

Typical normal values for PF range from 9.7 +/- 1.2mm [12]. Observe in Figure 10a that the right eye of the patient was actually looking towards her left because her face was not positioned correctly in front of the camera because no chin or head rest were used during data acquisition. The corresponding measurement is therefore smaller than normal. This problem can be easily solved by constraining the patient's head motion.

6. CONCLUSION

In this paper we have introduced a fast, robust, and accurate computer vision system to measure the palpebral fis-

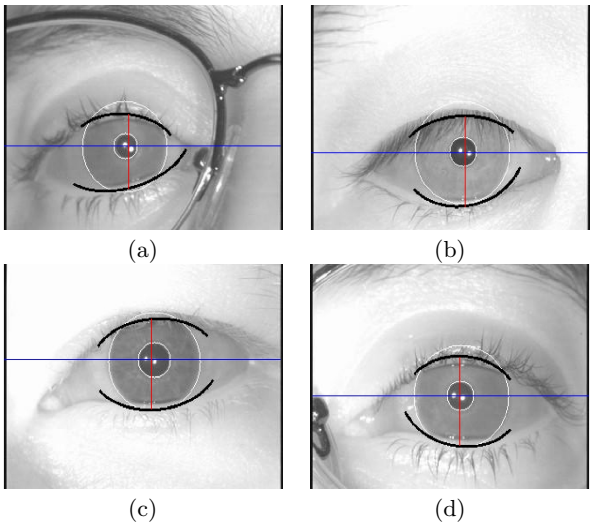

Figure 10: Results from the iris and eyelid segmentation. Observe that the system is robust to eyelashes and glasses.

	FP	uMDR	lMDR
(a)	163 / 8.2	68 / 3.4	95 / 4.8
(b)	196 / 9.8	79 / 4.0	117 / 5.9
(c)	198 / 9.9	87 / 4.4	111 / 5.6
(d)	194 / 9.7	86 / 4.3	108 / 5.4

Table 1: Measurements from Figure 10, in pixels / millimeters. All images were taken when the patient was about 55cm from the camera using a fixed focus lens. In this configuration, 200 pixels correspond to about 10mm.

sure (PF) and the upper and lower marginal reflex distances (MRDs). The system operates at video frame rates (30Hz) and automatically detects when the patient's eye is in the correct position. Currently the system's output is in pixels, and the conversion to millimeters is still manual, but this process is already being automated. Further experiments are required to assess if the accuracy of the system clinically acceptable, but the results presented in this paper are very encouraging.

Several extentions are possible using video processing, such as computing statistics of the measurements over a period of time, such as average and maximum PF or MRD, computing the eye blink rate, etc.

7. ACKNOWLEDGMENTS

The authors would like to thank FAPESP (Fundao de Amparo à Pesquisa do Estado de São Paulo) for their financial support.

8. REFERENCES

[1] A. Amir, D. Koons, M. Flickner, and C. Morimoto. Method and apparatus for determining eye contact. *IBM Docket no. AM9-98-137 (patente requerida)*, December 1998.

[2] K. Bobridis, A. Assi, A. Indar, C. Bunce, and A. Tyers. Repeatability and reproducibility of upper eyelid measurements. *British Journal of Ophthalmology*, 85:99–101, 2001.

[3] A. Cruz and A. Baccega. Analise bidimensional computadorizada da fenda palpebral. *Arq Bras Oftalmologia*, 64(1):13–19, 2001.

[4] A. T. Duchowski. A breadth-first survey of eye tracking applications. *Behavioral Research Methods, Instruments, and Computers*, pages 1–16, 2002.

[5] J. Holds. focus on digital external photography. *Rev Ophthalmol*, pages 78–81, 2001.

[6] E. B. Jr. Evaluation of the eyelids. In *Ophthalmic Plastic Surgery - Decision Making and Techniques*, pages 43–49. McGraw-Hill, 2002.

[7] E. B. Jr. Surgical anatomy of the eyelids. In *Ophthalmic Plastic Surgery - Decision Making and Techniques*, pages 25–41. McGraw-Hill, 2002.

[8] R. Kothari and J. Mitchell. Detection of eye locations in unconstrained visual images. In *International Conference on Image Processing*, volume I, pages 519–522, Lausanne, Switzerland, September 1996.

[9] S. Matayoshi. Anatomia cirúrgica. In *Manual de cirurgia plástica ocular*, pages 1–19, São Paulo, 2004. Roca.

[10] C. Morimoto, D. Koons, A. Amir, and M. Flickner. Pupil detection and tracking using multiple light sources. *Image and Vision Computing*, 18(4):331–336, March 2000.

[11] C. H. Morimoto, T. T. Santos, and A. S. Muniz. Automatic iris segmentation using active near infra red lighting. In *Proc. of the Simpósio Brasileiro de Computação Gráfica e Processamento de Imagens - SIBGRAPI*, pages 37–43, 2005.

[12] S. Read, M. Collins, L. Carney, and R. Iskander. The morphology of the palpebral fissure in different directions of vertical gaze. *Optometry & Vision Science*, 83(10):715–722, October 2006.

[13] B. Smith and F. Nesi. *Practical Techniques in Ophthalmic plastic surgery*. Mosby, St. Louis, 1981.

[14] E. Soares, A. Figueiredo, L. Oliveira, and M. M. aes. Blefaroptse. In *Cirurgia Plástica Ocular*, pages 77–152. Roca, 1997.

[15] G. Wyszecki and W. Stiles. *Color Science: Concepts and Methods, Quantitative Data and Formulae*. John Wiley & Sons, New York, 1982.